Photoinduced Micropatterning of Silver Nanoparticles in a Titanium Dioxide/Poly(acrylic acid) Alternate Thin Film

Suguru Kodaira,[1] Seung-Woo Lee,*[1] and Toyoki Kunitake[1,2]
[1]*Graduate School of Environmental Engineering, the University of Kitakyushu, 1-1 Hibikino, Kitakyushu 808-0135*
[2]*Frontier Research System (FRS), The Institute of Physical and Chemical Research (RIKEN), 2-1 Hirosawa, Wako 351-0198*

(Received November 13, 2007; CL-071257; E-mail: leesw@env.kitakyu-u.ac.jp)

Micropatterning of Ag nanoparticles was conducted with a Ag^+-incorporated TiO_2/poly(acrylic acid) (PAA) alternate ultrathin film by photochemical reduction through a patterned photomask. The prepared Ag nanoparticles possessed a mean diameter of 5.7 ± 1.7 nm.

Chemical patterning has attracted intense interests in many fields ranging from microelectronics to chemical and biological sensor applications. Various micropatterning approaches have been reported, and microcontact printing (μCP) and dip-pen nanolithography (DNP) techniques have been mainly used in patterning surfaces that are immobilized with a self-assembled monolayer (SAM).[1,2] Separately, the layer-by-layer (LBL) alternate films can be more effectively used in micropatterning.[3] A broad range of useful materials incorporated into LBL assemblies, such as biomolecules, nanoparticles, nanotubes, and synthetic polymers, offer us a great opportunity to explore new concepts for the preparation of functional thin films.

On the other hand, nanostructured metal oxide thin films are known to display advantages for designing unique chemical functions. The sol–gel method is one of the most important techniques for the fabrication of ultrathin films of metal oxides and metal oxide/organic hybrid materials. Over the last ten years, we have extensively studied the surface sol–gel process that is based on adsorption of metal alkoxide molecules from solution onto hydroxylated surfaces and subsequent hydrolysis to give nanometer-thick oxide films. Recently, this process has been expanded to the introduction of a variety of metal ions by the ion-exchange process and to the in situ preparation of silver and other noble metal nanoparticles.[4] Among others, TiO_2 gel films were efficient for reduction of Ag^+ ions since they have strong absorption at around 250 nm and are highly photoactive for UV light.[4,5] This approach would be much expanded if we use alternate layers of TiO_2 and polymers with functional groups like carboxylic and amino groups that are able to act as ligands to metal ions. In this study, we first examined the preparation of Ag nanoparticles by photochemical reduction of Ag^+ ions incorporated in a TiO_2/PAA (poly(acrylic acid)) alternate thin film and then explored micropatterning with a patterned mask (Figure 1a).

The TiO_2/PAA alternate film was assembled by the gas-phase surface sol–gel (GSSG) process[6] on a quartz substrate. First, Ti(O–^{n}Bu)$_4$, was heated in a sealed bottle at 85 °C, and the vaporized Ti(O–^{n}Bu)$_4$ was carried with nitrogen gas at a flow rate of 3 L/min. It was allowed to deposite on the quartz plate for 10 min, and the physisorbed alkoxide was removed by flushing nitrogen gas. Then, the quartz substrate was immersed in deionized water for 1 min and dried with nitrogen gas. Subsequently, the TiO_2 gel-deposited substrate was immersed in a 0.1 wt % aqueous solution of PAA (M_w: 250,000) for 20 min at 25 °C, rinsed with deionized water, and then dried with nitrogen gas. This alternate deposition of TiO_2 gel and PAA layers was repeated 10 times.

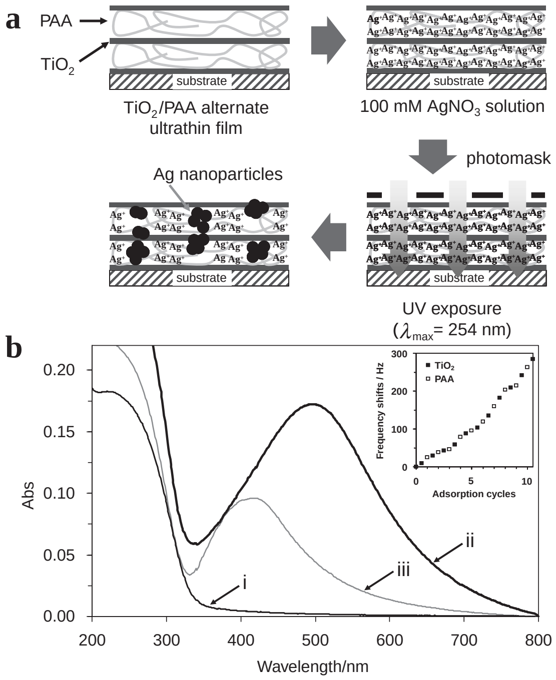

Figure 1. (a) Schematic illustration of photoinduced micropatterning and (b) UV–vis spectral changes of a $(TiO_2/PAA)_{10}TiO_2$ ultrathin film: (i) as-prepared and after (ii) photochemical ($\lambda_{max} = 254$ nm) and (iii) chemical (200 mM $NaBH_4$ in water) reduction of incorporated Ag^+ ions. The inset of Figure 1b shows QCM frequency changes due to alternate adsorption of Ti(O–^{n}Bu)$_4$ and PAA.

Figure 1b shows UV–vis absorption spectra of the alternate multilayers on a quartz substrate. The absorbance of TiO_2 gel in the near UV and visible regions increased in proportion to the adsorption cycle up to 10 cycles. The outermost surface was coated with a TiO_2 gel layer. The inset of Figure 1b shows QCM (9 MHz, 0.32 cm^2 for both sides) frequency changes due to the alternate adsorption. The QCM frequency linearly decreases with adsorption cycles, indicating regular growth of the TiO_2 gel/PAA multilayer film. Average frequency changes by the adsorption of Ti(O–^{n}Bu)$_4$ and PAA are 13 ± 8 and 14 ± 8 Hz, respectively. The thickness of each layer can be estimated by using Sauerbrey's equation.[7] The ΔF value of 13 Hz corresponds to a thickness increase of ca. 2 Å for the TiO_2 gel layer, using the density of bulk TiO_2 gel (1.7 g/cm^3).[8] Similarly, the thickness of the adsorbed PAA layer is estimated to be 3 Å, assuming a density of the PAA layer to be 1.4 g/cm^3.[9]

The film on a quartz plate was then immersed in aqueous $AgNO_3$ (100 mM) for 20 min, rinsed with pure water for 1 min, and dried by flushing nitrogen gas. Photochemical reduction of the incorporated Ag^+ ions was carried out with a UV light source of a UVG-54 Mineralight lamp (254 nm, UVP Upland, USA): the

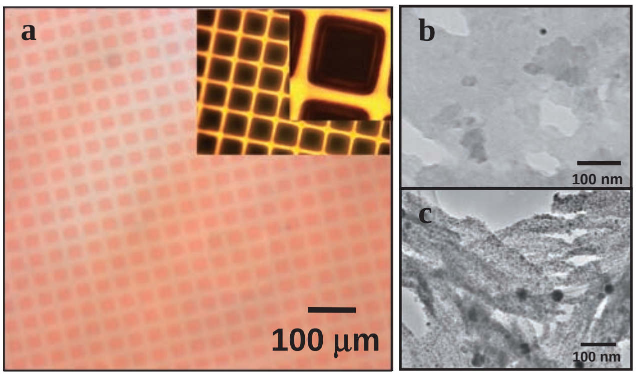

Figure 2. (a) Optical microscopic image of a Ag-micropatterned $(TiO_2/PAA)_{10}TiO_2$ ultrathin film. (b), (c) TEM images before and after photochemical reduction of incorporated Ag^+ ions by UV exposure ($\lambda_{max} = 254$ nm, 30 min). The inset of Figure 2a shows a TEM grid photomask (25 μm open squares separated by 17-μm lines).

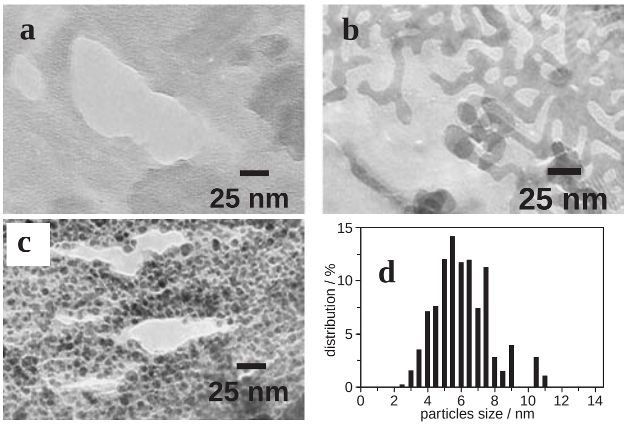

Figure 3. Magnified TEM images of a $(TiO_2/PAA)_{10}TiO_2$ ultrathin film: (a) as-prepared, (b) after $AgNO_3$ deposition for 20 min, and (c) after UV exposure for 30 min. (d) Size distribution of Ag nanoparticles obtained by photochemical reduction.

light intensity reaching the film was measured to be 0.78 mW/cm^2 by a light power meter (UVC-254, Custom, Japan). Curve ii in Figure 1b shows absorption spectrum of the Ag^+-incorporated thin film after photochemical reduction for 30 min. The peak observed at around 496 nm can be assigned to the surface plasmon resonance peak of spatially confined electrons in Ag nanoparticles. This band shows an unusually large red shift from a typical plasmon peak of Ag nanoparticles at 400 nm. This red shift may be related to close contact of adjacent silver particles.[4,10] On the other hand, chemical reduction was conducted by immersing the Ag^+-incorporated film in aqueous $NaBH_4$ (200 mM) for 10 min, followed by rinsing in pure water for 1 min and drying with N_2. The resulting Ag surface plasmon peak was located at 416 nm and was relatively narrow (curve iii in Figure 1b). He et al. reported that Ag^+ ions could be lost into aqueous $NaBH_4$ by ion exchange, when $NaBH_4$ is used as the reductant.[4] Anyway, this means that the smaller Ag nanoparticle of narrow distribution was prepared with $NaBH_4$.

Photochemical reduction of metal ions would be more interesting if it is associated with micropatterns. Figure 2a shows an optical microscopc image of the Ag^+-incorporated TiO_2/PAA alternate film patterned by UV exposure (254 nm, 30 min) through a TEM grid photomask (25-μm open squares separated by 17-μm lines). Before UV exposure, the film was colorless, transparent, and smooth and had a thickness of ca. 5 nm. Patterns prepared by UV exposure are very clear and completely reflect the figure of the TEM photomask. Regions that were shielded by the grid show no change in color, while UV-exposed regions became darker. This suggests that Ag nanoparticles were prepared only in the exposed region. To confirm this fact, we carried out TEM observation before and after UV exposure. The separately prepared UV-exposed and UV-unexposed films were scratched off from their quartz substrates in H_2O and transferred to a TEM grid by a dispenser. The TEM observations in Figures 2b and 2c show a clear difference between the two films.

Figure 3c shows a magnified TEM image of the UV-exposed sample. Ag nanoparticles are clearly seen. The mean diameter of the particles and their standard deviation were calculated to be 5.7 ± 1.7 nm (Figure 3d), which is smaller than the reported value (7.6 ± 3.0 nm) for the ion-exchanged TiO_2 film.[4] However, the current method has a much larger red shift of the surface plasmon resonance peak, compared with the ion-exchange process. Perhaps, this red shift may be attributed the close contact of Ag nanoparticles in the PAA layer, as expected from the UV–vis data (Figure 1b). This result can be evident from the metal composition of Ag/Ti (1.4:1) by XPS (see Figure S1), which is 1.7 times bigger than that for the ion-exchanged TiO_2 film.[4]

In conclusion, we examined the preparation of Ag nanoparticles by photochemical reduction of the Ag^+-incorporated TiO_2/PAA alternate thin film and explored micropatterning using a patterned mask. The micropatterns prepared by UV exposure were very clear and completely reflected the figure of the mask. Close contact of Ag nanoparticles that was attributed to the densely assembled PAA layers caused a large red shift of the surface plasmon resonance peak. An advantageous feature of the current micropatterning technique is that Ag^+ ions in UV-unexposed regions can be readily removed by the treatment with acids or chelating agents and substituted with other metal ions. The general applicability of the present approach is noteworthy, and various chelating polymers may be used for this approach. Therefore, the current method will be useful in the preparation of homo- and hetero-metallic patterns based on metal oxide thin films.

This work was supported by a Grant-in-Aid for Science Research (No. 17651075) from the Ministry of Education, Culture, Sports, Science and Technology of Japan and by the MEXT via the Kitakyushu Knowledge-based Cluster Project.

References and Notes

1 A. Kumar, G. M. Whitesides, *Science* **1994**, *263*, 60; Y. Xia, J. A. Rogers, K. E. Paul, G. M. Whitesides, *Chem. Rev.* **1999**, *99*, 1823.
2 R. D. Piner, J. Zhu, F. Xu, S. Hong, C. A. Merkin, *Science* **1999**, *283*, 661; D. S. Ginger, H. Zhang, C. A. Merkin, *Angew. Chem., Int. Ed.* **2004**, *43*, 30.
3 J. Hiller, J. D. Mendelsohn, M. F. Rubner, *Nature Mater.* **2002**, *1*, 59; S. C. Olugebefola, S.-W. Ryu, A. J. Nolte, M. F. Rubner, A. M. Mayes, *Langmuir* **2006**, *22*, 5958; S. W. Lee, R. G. Sanedrin, B.-K. Oh, C. A. Mirkin, *Adv. Mater.* **2005**, *17*, 2749; Z. Liang, Q. Wang, *Langmuir* **2004**, *20*, 9600.
4 J. He, I. Ichinose, T. Kunitake, A. Nakao, *Langmuir* **2002**, *18*, 10005; J. He, I. Ichinose, T. Kunitake, A. Nakao, Y. Shiraishi, N. Toshima, *J. Am. Chem. Soc.* **2003**, *125*, 11034.
5 K. Naoi, Y. Ohko, T. Tatsuma, *J. Am. Chem. Soc.* **2004**, *126*, 3664; Y. Zhou, R. Ma, Y. Ebina, K. Takada, T. Sasaki, *Chem. Mater.* **2006**, *18*, 1235; E. Haro-Poniatowski, E. Fort, J. P. Lacharme, C. Ricolleau, *Appl. Phys. Lett.* **2005**, *87*, 143103.
6 D.-H. Yang, N. Takahara, N. Mizutani, S.-W. Lee, T. Kunitake, *Chem. Lett.* **2006**, *35*, 990.
7 G. Sauerbrey, *Z. Phys.* **1959**, *155*, 206.
8 I. Ichinose, H. Senzu, T. Kunitake, *Chem. Lett.* **1996**, 831; I. Ichinose, H. Senzu, T. Kunitake, *Chem. Mater.* **1997**, *9*, 1296.
9 I. Ichinose, T. Kawakami, T. Kunitake, *Adv. Mater.* **1998**, *10*, 535.
10 H. Fujiwara, S. Yanagida, P. V. Kamat, *J. Phys. Chem. B* **1999**, *103*, 2589.
11 Supporting Information is available electronically on the CSJ-Jounal web site, http://www.csj.jp/journals/chem-lett/.

Published on the web (Advance View) January 12, 2008; doi:10.1246/cl.2008.168